LITERATURE CITED

1. Yu. S. Kachanov, V. V. Kozlov, and V. Ya. Levchenko, Origin of Turbulence in Boundary Layer [in Russian], Nauka, Novosibirsk (1982).
2. V. N. Zhigulev, "Determination of critical Reynolds number for transition from laminar to turbulent boundary layer," in: Mechanics of Continuous Media [in Russian], Inst. of Theoretical and Applied Mechanics, Siberian Branch, Academy of Sciences of the USSR, Novosibirsk (1981).
3. L. B. Aizin and N. F. Polyakov, Generation of Tollmien–Schlichting Waves by Sound on Isolated Surface Roughness by Fluid Flow [in Russian], Preprint No. 17, Inst. of Theoretial and Applied Mechanics, Siberian Branch, Academy of Sciences of the USSR, Novosibirsk (1979).
4. A. I. Ruban, "Generation of Tollmien–Schlichting waves by sound," Izv. Akad. Nauk SSSR, Mekh. Zhidk. Gaza, No. 4 (1984).
5. N. A. Zavol'skii, V. P. Reutov, and G. B. Rybushkina, "Excitation of Tollmien–Schlichting waves with acoustic scattering and vortex perturbations in boundary layer on wavy surface," Zh. Prikl. Mekh. Tekh. Fiz., No. 3 (1983).
6. V. N. Zhigulev, N. V. Sidorenko, and A. M. Tumin, "Generation of unstable waves in boundary layer by external turbulence," Zh. Prikl. Mekh. Tekh. Fiz., No. 6 (1980).
7. A. M. Tumin and A. V. Fedorov, "Spatial growth of disturbances in compressible boundary layer," Zh. Prikl. Mekh. Tekh. Fiz., No. 4 (1983).
8. V. N. Zhigulev, "Excitation and growth of instability in three-dimensional stationary boundary layers," Zh. Prikl. Mekh. Tekh. Fiz., No. 4 (1983).
9. A. V. Fedorov, "Excitation of unstable waves in compressible boundary layer due to acoustic field," Chisl. Metody Mekh. Splosh. Sred., 13, No. 3 (1982).
10. A. V. Fedorov, "Excitation of the Tollmien–Schlichting waves by the acoustic disturbances in the compressible boundary layer," in: Proc. IUTAM Symp., Springer, Berlin (1985).
11. V. V. Bogolepov and V. Ya. Neiland, "Supersonic viscous flow past small roughnesses on the surface of the body," Trudy Central Aero-Hydrodynamic Institute (TsAGI), Vol. 1363 (1971).
12. S. A. Gaponov and A. A. Maslov, Growth of Disturbances in Compressible Flows [in Russian], Nauka, Novosibirsk (1980).

DYNAMICS OF LAMINAR VORTEX RINGS IN A STRATIFIED LIQUID

V. S. Belyaev, A. M. Savinkov, and Yu. D. Chashechkin

UDC 532.527

The study of isolated vortices and interacting vortical structures on different scales (the principal structural elements in developed turbulence) is a traditional problem of fluid dynamics. In recent years there has been substantial progress in explaining the nature of the stability of vortices resulting from the stabilizing effect of centrifugal forces which suppress transport in the radial direction [1]. It has been established experimentally that there is a laminar core inside turbulent vortex rings [2]. A survey of theoretical and experimental studies of the motion of vortices in a uniform fluid was made in [3]. The dynamics of an isolated vortex is determined to a significant extent by the involvement of the surrounding fluid in the circulating motion and the loss of vorticity in the wake.

The question of the stability and evolution of a vortex in a stratified fluid is more complex. In this case, centrifugal forces are jointed by buoyancy, which suppresses motion in the vertical direction. Most experimental studies have investigated the vertical motion of vortex rings in a nonuniform fluid [4], modeling the motion of thermals in a stratified atmosphere [5, 6], vortex cores behind an airplane wing [7, 8], and structural elements of free turbulent flows [9]. The authors of [10] visualized a laminar vortex ring moving along the interface of mixing fluids. The interaction of an obliquely-moving vortex ring with a

Moscow. Translated from Zhurnal Prikladnoi Mekhaniki i Tekhnicheskoi Fiziki, No. 1, pp. 37-47, January-February, 1987. Original article submitted December 6, 1985.

 0021-8944/87/2801-0034$12.50

shock wave was studied experimentally in [11]. It follows from analysis of the phenomenological and numerical models used that a vortex ring moving along an interface should be inclined and lie horizontal [12]. The goal of the present study is to experimentally investigate the dynamics and structure of laminar vortex rings in a fluid with a linear density distribution.

1. The experiments were conducted in a rectangular basin measuring 140 × 40 × 46 cm. The side walls of the basin were made of optical glass. The basin was filled layer by layer with an aqueous solution of table salt of variable concentration. The thickness of the layers was 4 cm. Two days after the basin was filled, molecular diffusion had smoothed the stepped density profile. The uniformity of the gradient was checked with a shadowgram (the method of a vertical or horizontal slit – Foucault knife-edge) by means of a density marking [13]. The uniformity of the gradient was also checked by means of the distribution of electrical resistivity as measured with a microcontact transducer [14]. The flow pattern was visualized with an IAB-451 shadowgraph, with recording by an IKSR motion picture camera or an automatic RFK-5 photographic camera with speed from 4 to 10 frames/sec and 1/250 sec. The geometric characteristics of the vortices were measured from the shadowgram films with a STECOMETER stereo comparator (German Democratic Republic) with an error (allowing for the scale of the image) of ±4%. The amplitudes of the internal waves were measured with a "single-electrode" conductivity sensor [14] with an error no greater than ±10%.

The vortices were created by ejecting the fluid from a metal tube bent at a right angle. The delivery part of the tube was positioned horizontally. The accuracy of its placement was checked with a KO-10 optical quadrant with an error of ±20'. A cylindrical nozzle with an outlet opening 0.75 and 1 cm in diameter was fitted on the end of the tube. The ejecting piston was placed in the surface part of the generator and was put in motion by a spring. Both the degree of compression and length of travel of the spring could be regulated. The quantity of fluid discharged and the initial velocity and diameter of the vortex depended on the height of the water in the tube and the length and velocity of the piston. By regulating these quantities, we succeeded in obtaining vortex rings with prescribed initial parameters. The error of reproducibility of the initial velocity of the ring was ±5%. An additional grate was installed inside the horizontal part of the tube to obtain slow laminar rings. The tests were conducted in liquid with a linear density distribution with a buoyancy period T_k = 3-15 sec.

The shadowgrams were used to measure the following parameters of the vortex ring: the path traveled x (determined from the sharp leading edge of the vortex); translational velocity U; diameter D (the maximum vertical distance between the layers with a sharp density gradient on the outside boundary of the vortex). An "Élektronika D3-28" computer was used to perform a least-squares approximation of the test data with power and exponential relations. The representation was chosen on the basis of the condition of the maximum of the correlation coefficient and the minimum of the dispersion of the deviations. The main dimensionless characteristics were: the local Reynolds number $Re = U(x)D(x)/\nu$; the internal Froude number $Fr = U^2(x)T_k^2/4\pi^2D^2(x)$ (ν is the kinematic viscosity, equal to 0.01 cm/sec). In our tests, the initial velocity of the vortex U_0 = 2.5-20 cm/sec, while the initial values of the dimensionless characteristics Re_0 = 300-3200 and Fr_0 = 0.65-840. Laminar and turbulent rings were seen in this range of parameters. We did not systematically study the effect of stratification on stability of motion in the ring, but it can be stated qualitatively that a horizontally moving ring will be laminar if $Re_0 < 1000$. In a uniform liquid, a laminar ring is stable at $Re_0 < 600$, is unstable and disintegrates with the formation of a new, stable ring at $Re_0 \gtrsim 1000$, and becomes unstable from the very beginning at $Re_0 \sim 20{,}000$ [15]. Stratification somewhat stabilizes motion in the ring. At $1000 < Re_0 < 3000$, a ring moving as a whole becomes partially turbulent, the spiral structure is disturbed, and there is mixing of the liquid in the ring and the wake. At $Re_0 > 3000$, the ring is completely turbulent.

2. When the liquid is forced out on the sharp edge of the generator, the boundary layer separates and rotates into a spiral which becomes the main core of the forming vortex. At this stage, the distance between the centers of vorticity is roughly equal to the diameter of the discharge opening. After $t \approx 0.2$ sec, the spiral is twisted around the core and the streamline is closed, forming the atmosphere of the ring. During this time, the ring travels a distance roughly equal to its diameter. The ring moves without a change in dimensions and with almost no decrease in velocity for a period of 0.5-0.7 sec in the initial stage of the trajectory.

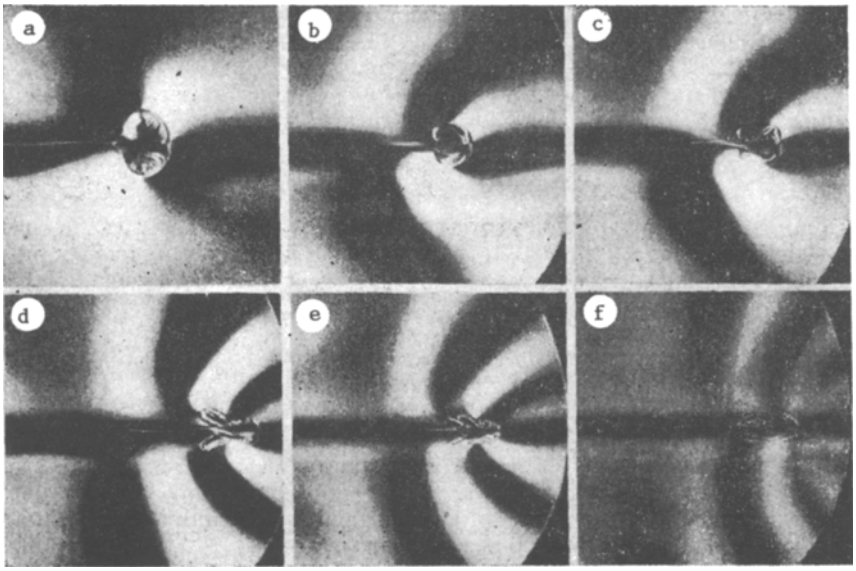

Fig. 1

The structure of the laminar ring at later stages of its motion is shown in Fig. 1 (the initial diameter of the formed ring D_0 = 1.47 cm, U_0 = 2.5 cm, T_k = 3 sec, Re_0 = 366, Fr_0 = 0.65). At the main stage of motion (Fig. 1a, t = 1.8 sec), the structure of the flow is similar to that seen in a uniform liquid [15, 16]. A thin toroidal core and an atmosphere around this core can be distinguished in the shadowgram. The form of the vortex ring resembles an ellipsoid with a regular spiral internal structure. The front part of the ring is more convex. The diffuse dark (in the second and fourth frames) and light (in the first and third frames) bands are internal waves. Their amplitude is small at this stage of motion, and with the chosen instrument sensitivity they are recorded only at distances comparable to the diameter of the ring. A thin light streak is visible behind the vortex along the line of motion. The density gradient in this streak exceeds the density gradient in the undisturbed medium – a density wake of 1-1.5 mm thickness. A conical projection is seen in the region of contact with the density wake on the rear surface of the vortex.

A thin, annular bound vortex is formed near the edge of the discharge opening. The diameter of this vortex is 1.5 times greater than the diameter of the shed vortex. Thin funnel-shaped striae connect the atmosphere of the bound vortex with the laminar density wake of the outgoing ring. The bound vortex subsequently slowly disintegrates, with the formation of an annular structure of density discontinuities near the edge of the generator. The nonsteady motion of the liquid in the ring formation region creates a system of transient conical internal waves of low (compared to the other type of internal waves) amplitude. The vertical dimension of the ring initially increases and then begins to decrease. At the end of this stage, the ring is rapidly slowed and generates internal waves.

Figure 1b shows the pattern of the vortex at the stage of intensive wave deceleration (t = 5 sec). The vortex loses its elliptical form, a fin is formed on its outside surface, the rear edge becomes planar and then concave, the laminar wake expands, and the spiral structure inside the vortex is shifted toward its periphery. The region of sharp gradients of the refractive index n and density ρ (in an aqueous solution of NaCl, these values are linked by the linear relation $\partial n/\partial z = 0.231 \partial\rho/\partial z$ [13]) is shifted toward the external boundary of the vortex. At this stage, the vortex intensively generates internal waves having a phase structure which is similar to that of bound internal waves [17]. Due to deceleration, the velocity of the vortex ring decreases and there is a simultaneous reduction in the length of the generating wave.

The flow inside the ring degenerates as translational velocity decreases, and the form of the flow begins to have a significant effect on the field of internal waves which is emitted. The waves stretch the ring in the region of the crests and compress it in the vicinity of the troughs. Thin density striae remaining from the ring atmosphere are curved accordingly (Fig. 1c, t = 6 sec). The remains of the atmosphere move slowly into the undisturbed medium. Here, the diameter of the lead part remains unchanged.

TABLE 1

x, cm	U, cm/sec	t, sec	K	ξ	η_*, mm	λ_0	$\lambda_1/2$	$\lambda_1'/2$	$\lambda_2/2$	$\lambda_2'/2$	$\lambda_3/2$	$\lambda_3'/2$
			$\eta(\tau)=Ke^{-\xi\tau}$, mm			cm						
7,5	3,5	1,4	0,12	0,30	0,142	15,75	2,1	—				
							—	1,8				
9,5	2,9	2,0	0,15	0,27	0,187	13,05	2,2	—				
							—	2,5				
11,5	2,3	2,8	0,18	0,22	0,221	10,35	2,5	—				
							—	3,1				
13,5	1,9	3,6	0,30	0,19	0,322	8,55	3,1	4,2				
							—	3,1				
15,5	1,3	5,0	0,39	0,19	0,393	5,85	2,0	4,1				
							—	3,0				
17,5	1,0	6,6	0,56	0,22	0,468	4,5	1,7	3,3	3,0			
							—	2,9	—			
19,5	0,8	8,2	0,53	0,23	0,459	3,6	1,6	2,8	3,3			
							—	2,2	—			
21,5	0,45	11,4	—	—	0,382	2,0	1,1	2,2	2,6	4,0		
							1,7	1,7	3,0	2,5		
23,5	0,1	16,5	—	—	0,307	0,45	0,5	1,5	1,8	2,1	2,5	3,7
							1,0	0,9	1,8	1,9	2,5	2,5

The diameter of the lead part subsequently decreases (with individual elements of the spiral structure being visible on the periphery of the cluster), while the rear part of the ring continues to expand, forming the characteristic conical structure (Fig. 1d, t = 9 sec). This form of the disintegrating ring is stable and was seen in all of the tests with different stratifications. It exists for 2-3 sec. The side of the cone is subsequently pressed toward the axis of motion, and the form of the boundary of the cluster becomes more irregular (Fig. 1e, t = 10 sec). Its vertical dimension pulsates over time in synchronicity with variations of density on the boundary of the cluster which are initiated by the waves. After long periods of time (t > 10 sec), the vortex is nearly stopped (U < 0.1 cm/sec), and the remains of its atmosphere exist in the form of a system of annular and conical striae (Fig. 1f, t = 15 sec). At this stage, internal waves cease to be generated, and the amplitude of these waves in the vicinity of the cluster is smaller than the amplitude of earlier-generated waves located some distance from the cluster. The form of the wave fronts gradually acquires the conical shape typical of short transient internal waves of the Cauchy–Poisson type. At later stages, the remains of the ring slowly diffuse into the surrounding medium and disappear without a change in form.

Mixing of the liquid inside the ring disturbs the initial density distribution, and after decay of the motions along the entire path of the ring there remains a column of liquid with a diameter equal to the diameter of the discharge hole. The density gradient inside this column is less than in the surrounding medium; it is manifest in the form of a dark horizontal band on the shadowgrams. A zone in which the density gradients are higher than the initial values is located between two cylindrical surfaces with an inside diameter d_c = d and an outside diameter $D_c \approx 2d$, where d is the diameter of the discharge hole of the vortex generator. The outer boundary of the region of perturbed gradients is readily visible (Fig.

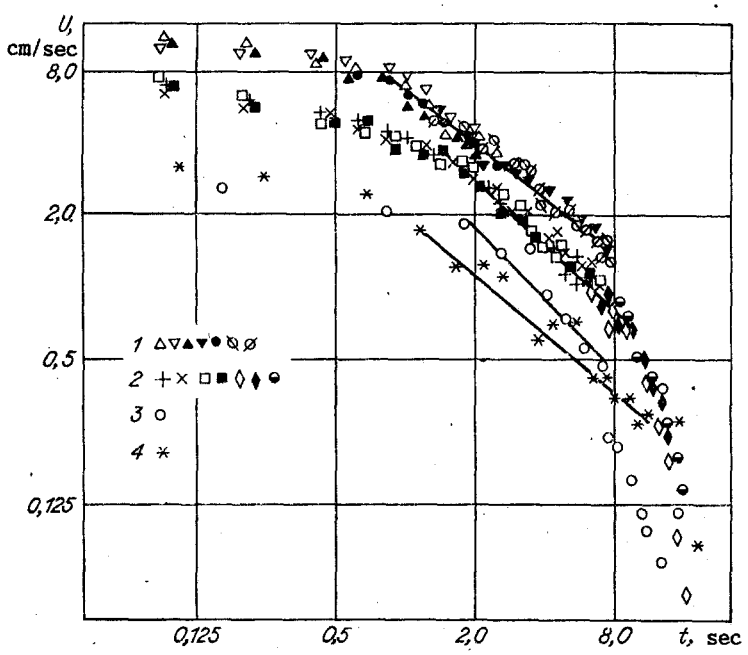

Fig. 2

TABLE 2

T_k, sec	U_0, cm/sec	A	α	B	β	t_+, sec	L, cm	D_0, cm	C	γ	D_*, cm	D_*/D_0	t_*, sec	τ_*
		$U(t)=At^{-\alpha}$, cm/sec		$U(x')=Be^{x(-\beta x')}$, cm/sec					$D(t)=Ct^{\gamma}$, cm, $t<t_*$					
3	2,5	4,9	1,21	9,5	0,28	11	12	1,47	1,5	0,0004	1,5	1,02	2,0	0,67
	3,84	5,1	0,95	5,2	0,11	(10)	(15,5)	1,4	1,5	0,04	1,65	1,18	2,5	0,83
	13	5,9	0,62	16,2	0,09	16	33	1,4	1,9	0,19	2,4	1,7	2,6	0,87
4,5	6,5	5,2	0,85	10,0	0,13	17	23	1,2	1,3	0,15	1,65	1,375	4,5	1,0
	10,6	6,0	0,7	14,4	0,08	—	—	1,5	1,7	0,17	2,3	1,53	4,5	1,0
10	3,13	1,9	0,79	4,6	0,21	16	11,5	0,96	1,0	0,12	1,35	1,4	11	1,1
15	20	10,1	0,77	25,2	0,06	(10)	(49)	1,6	1,8	0,25	3,3	2,06	—	—

1) and is also evident in micrographs of the shadowgrams. Relict striated laminar structures – residues of the ring atmosphere – exist for a period of 100-150 sec. Smoother large-scale density perturbations exist for 6-8 h.

Table 1 shows the variation of the length of the internal wave generated as the ring advances. The table shows values of the half-length of the wave $\lambda/2$ – the distance between an adjacent crest and trough for the top and bottom half-spaces (the width of the corresponding dark or light band on the shadowgrams). The wave number is reckoned from the leading edge of the vortex, $\lambda_0 = U(x)T_k$ is the running value of the length of the bound internal wave [17].

3. Four sections can be distinguished in the motion of a vortex ring in a stratified liquid along a horizontal trajectory: an initial section (including the stage of ring formation); a main stage (exponential dependence of velocity on the distance travelled and power dependence of velocity on time); intensive wave deceleration; disintegration. On the initial section, with a duration of 0.3-0.5 sec, the velocity and size of the ring remain nearly constant. The duration of the main section depends on the velocity and amounts to 5-7 sec.

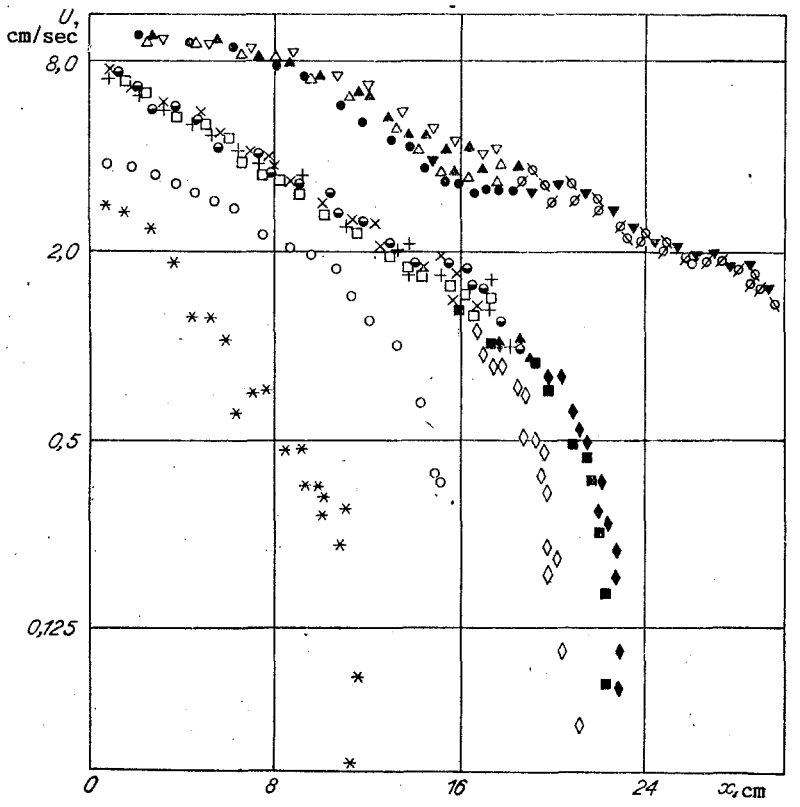

Fig. 3

During this time, the ring traverses much of its total path (70-90%). On the relation U(t) shown in double-log coordinates in Fig. 2, this section is represented by a straight line (variants 1-4 correspond to T_k = 4.5, 4.5, 3, and 10 sec, u_0 = 10.6, 6.5, 2.5, and 3.13 cm/sec; the different symbols denote different realizations with the same initial conditions). Measurements were stopped at x > 30 cm for variant 1, since the partly turbulent ring (Re_0 = 1600) moved outside the field of view of the shadowgraph. The evolution of the remaining rings was followed until they stopped completely. On the main section, the relation U(t) is approximated by the formula $U(t) = At^{-\alpha}$ (cm/sec), where the coefficients A and α are determined by the least-squares method. Values of these coefficients are shown in Table 2. The exponent α decreases with an increase in the velocity and the buoyancy period. In a uniform liquid for $Re_0 < 600$, $\alpha = 1$ [15]. On the section of active wave deceleration, the relation U(t) is exponential. Later, during the stage of disintegration of the ring, the relation is more accurately approximated by the power relation $U(t) = A_+t^{-\alpha+}$ (cm/sec), α_+ = 4.3.

Figure 3 shows the dependence of velocity on the path travelled in a semilogarithmic scale (the values of the parameters for 1, 2, and 4 coincide with the corresponding parameters in Figs. 2 and 3 – T_k = 3 sec, U_0 = 3.84 cm/sec). The notation for variants 1-4 is the same as in Fig. 2. The main section is approximated by the relation $U(x') = B\exp\{-\beta x'\}$, where x' = x/d. The coefficients B and β, determined by the least-squares method, are shown in Table 2. The character of the relation U(x') is consistent with the relation measured in the uniform liquid. The coefficient β, calculated from Fig. 5 [15], is equal to 0.19. On the deceleration section, $U(x') = B_+\exp\{-\beta_+x'\}$ (cm/sec). Meanwhile, the exponent increases to β_+ = 0.55, 0.53, and 0.62 (variants 2-4).

The relations U(t) and U(x) are smooth on the initial section, while velocity changes suddenly on the main section. These changes increase with an increase in the initial velocity of the ring and the length of the path. Such fluctuations are associated mainly with the change in form and with pulsation of the geometric dimensions of the ring. The period of the pulsations is 0.1-0.2 sec for the horizontal dimensions and 0.8-1.2 sec for the vertical dimensions.

Figure 4 shows the dependence of the vertical dimension of the ring on time in liquids with different buoyancy periods (T_k = 15, 10, and 4.5 sec; U_0 = 20, 3.13, and 6.5 cm/sec –

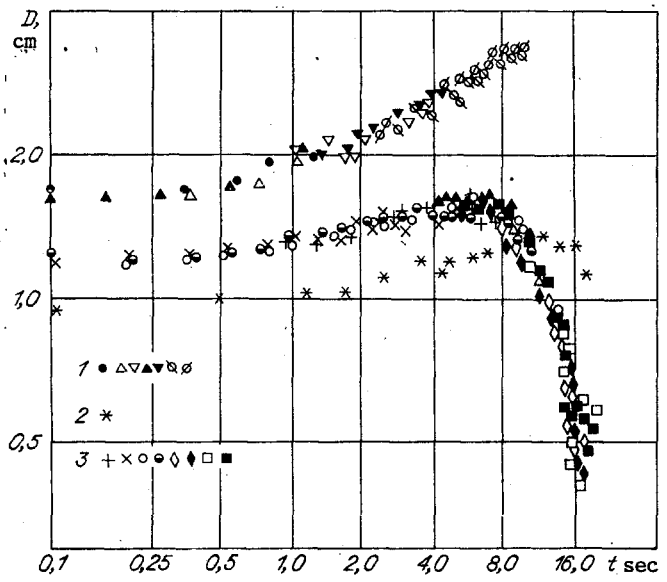

Fig. 4

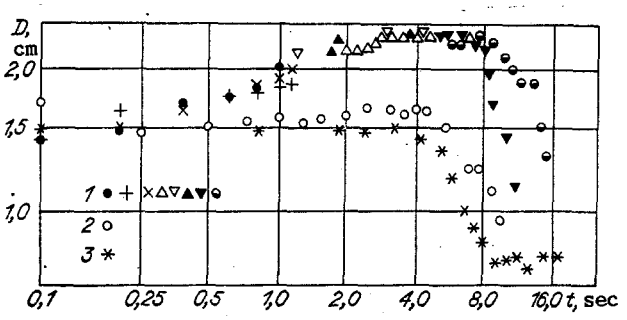

Fig. 5

variants 1-3). The different symbols on each curve denote individual realizations with the same initial velocities. It can be seen from Figs. 2 and 3 that there is an initial section ($t < 0.5$ sec) on which the size of the ring remains nearly constant; there is also a section on which the size of the ring remains nearly constant; there is also a section on which the vertical dimension of the ring increases (0.5 sec $< t < t_*$, where t_* is the time of cessation of diameter increase) and on which $D(t)$ is approximated by the formula $D(t) = Ct^{\gamma}$ (cm) (the values of the coefficients C and γ and the time t_* are shown in Table 2); also present is a section of motion with a constant diameter (duration 2-3 sec); finally, there is a section associated with collapse and disintegration of the ring. This section begins at the stage of active deceleration. The duration of the stage in which the dimensions of the ring increase itself increases with an increase in the buoyancy period of the medium. On the collapse section, the vertical dimension of the ring decreases exponentially with time: $D(\tau) = C_+ \exp\{-\gamma_+\tau\}$ (cm), where $\tau = t/T_k$ (for 2 in Fig. 4 at $t > 8$ sec, $C_+ = 2.0$, $\gamma_+ = 0.3$; for 3 at $t > 7$ sec, $C_+ = 2.5$, $\gamma_+ = 0.34$). The dependence of the vertical dimension of the ring on the path travelled is similar to that shown in Fig. 4. On the section of ring expansion, $D(x') = M\exp\{\kappa x'\}$ (cm), where for $T_k = 4.5$ sec, $U_0 = 6.5$ cm/sec, $M = 1.1$, $\kappa = 0.03$; in the collapse phase, $D(x') = M_+ \exp\{-\kappa_+ x'\}$ (cm), where for the same initial conditions $M_+ = 22.3$, $\kappa_+ = 0.15$. The maximum distance travelled by these rings is 21-23 cm. The relative scatter lies within the range ±10%, which is consistent with the error of reproducibility of the initial velocity of the ring. For variant 2, $M = 0.89$, $\kappa = 0.02$, $M_+ = 6.0$, $\kappa_+ = 0.08$.

With an increase in the initial velocity of the ring in the liquid with $T_k = 3$ sec, there is some reduction in its initial diameter, an increase in the maximum size of the ring (which is evidence of an increase in the involvement of the surrounding liquid in the vortical motion), and an increase in the length of the phase of motion with the maximum vertical dimension (Fig. 5, $T_k = 3$ sec, variants 1-3 at $U_0 = 13$, 3.84, and 2.5 cm/sec). The time until attainment of the maximum vertical dimension t_* also increases with an increase in velocity

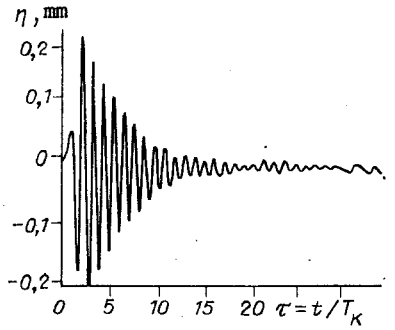

Fig. 6

(see Table 2). At the stage of expansion of the ring, its vertical dimension $D(t) = Ct^{\gamma}$ (cm), where the exponent increases appreciably with an increase in velocity (from 0.0004 to 0.19, Table 2). At the deceleration stage, $D(\tau) = C_+ \exp\{-\gamma_+\tau\}$ (cm), where $C_+^{(1)} = 4.9$, $\gamma_+^{(1)} = 0.3$, $C_+^{(2)} = 2.5$, $\gamma_+^{(2)} = 0.3$, $C_+^{(3)} = 2.2$, $\gamma_+^{(3)} = 0.3$ – variants 1-3. The exponent $\gamma_+ = 0.3$ ($t > t_*$) is nearly independent of the initial velocity and the buoyancy scale. The graph of $D(x')$ can be approximated by an exponential relation both for the expansion stage and for the collapse stage (for 1, $M = 1.3$, $\kappa = 0.036$, $M_+ = 15.2$, $\kappa_+ = 0.07$; 2, $M = 1.4$, $\kappa = 0.014$, $M_+ = 13.6$, $\kappa_+ = 0.17$; 3, $M = 1.5$, $\kappa = 0.00009$, $M_+ = 17.1$, $\kappa_+ = 0.27$).

Measurements of the vertical displacements of particles caused by the internal waves were made in the vertical plane passing through the line of motion of the center of the ring at the height $z = 3.0$ cm at different distances from the nozzle edge. Figure 6 shows a typical record of these displacements ($T_k = 4.5$ sec, $U_0 = 8.5$ cm/sec, the coordinates of the measurement points 21.5, 0, 3 cm). The dependence of the vertical displacement η on the dimensionless quantity τ is oscillatory in character with a constant frequency and an exponentially decaying amplitude. In the liquid with $T_k = 4.5$ sec, the period of the oscillations is $T = 4.9$ sec and remains at this value with increasing distance from the nozzle edge (the duration of the first seven oscillations is 34.25 sec for $x = 7.5$ and 17.5 cm). Table 1 shows values of the coefficient ξ in relation to $\eta(\tau) = K\exp\{-\xi\tau\}$ (mm) ($\tau = t/T_k$) at different distances from the hole, with the maximum displacement of the particles in the first crest and trough η_*, the length of the bound internal wave $\lambda_0 = U(x)T_k$, and wave half-lengths measured from the shadowgrams ($T_k = 4.5$ sec, $U_0 = 6.5$ cm/sec). The coefficient K increases with increasing distance from the source, while the exponent ξ is minimal at $x \approx 15.5$ cm. The wavelength becomes comparable to λ_0 at $x > 17.5$ cm, where $Fr < 0.25$. The damping factor ξ exceeds the calculated value for bound internal waves [17] when it is estimated by using the measured wavelengths. This difference can be attributed to the short duration of the

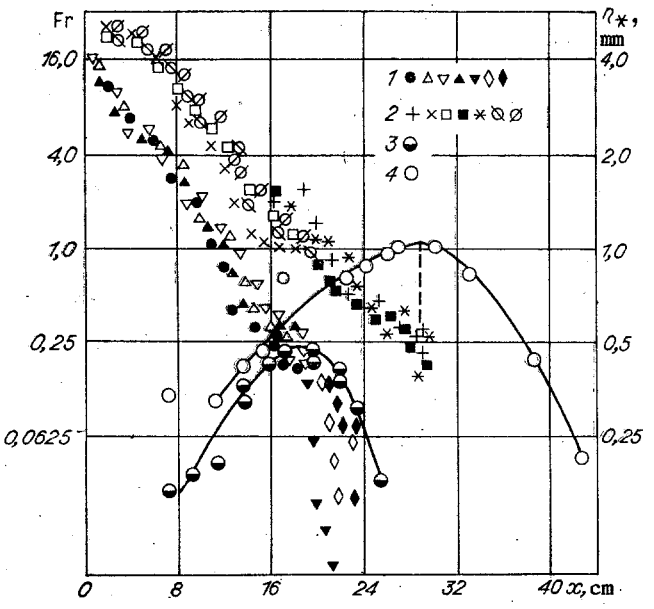

Fig. 7

stage of active wave deceleration. The ring acts as a generator of internal waves for a relatively short period of time.

This conclusion is supported by an examination of the dependence on the distance to the source of the local value of Fr and the maximum recorded displacement of the particles in an adjacent crest and trough (Fig. 7, T_k = 4.5 sec). On the main section $Fr(x') = E\exp\{-\mu x'\}$, E_1 = 13, μ_1 = 0.23, U_0 = 6.5 cm/sec (variant 1, x < 20 cm), E_2 = 26, μ_2 = 0.18, U_0 = 10.6 cm/sec (variant 2, x < 28 cm). Also shown here is the dependence of the maximum range of particle displacement η_* on the distance to the discharge hole x over which the measurements were made. Here, T_k = 4.5 sec, d = 1 cm, and the initial parameters remained the same (3, 4 for U_0 = 6.5 and 10.6 cm/sec). The intensity of wave generation increases with increasing distance of the ring from the source and reaches a maximum at those points of the trajectory near which the local internal Froude number is equal to 0.25. The maximum increases with a decrease in the initial velocity of the vortex. The maximum amplitude of the internal waves increases with an increase in initial velocity.

Table 2 shows the main characteristics of the investigated rings. The table shows the limiting lifetime of a ring t_+ (at $t > t_+$, the translational velocity of the ring is less than 0.1 cm/sec; for the values shown in the brackets, this velocity exceeds the above value), the distance travelled L (determined similarly to t_+), the initial diameter of the ring D_0, the maximum diameter D_*, and the time until attainment of the maximum diameter t_*, $\tau_* = t_*/T_k$.

On the main section of ring motion, the exponent α in the relation $U(t) = At^{-\alpha}$ decreases with an increase in velocity for the given stratification. There is a corresponding decrease in the coefficient β in the relation $U(x') = B\exp\{-\beta x'\}$. The limiting lifetime of the ring t_+ and the distance it travelled L increase with an increase in the initial velocity. The initial diameter D_0 is slightly dependent on the dimensional parameters of the problem (U_0 and T_k). The exponent γ in the relation $D(t) = Ct^{\gamma}$ increases significantly with an increase in ring velocity, and there is a simultaneous increase in the maximum vertical dimension D_*. The time until attainment of the maximum diameter (t_*, τ_*) increases with an increase in the initial velocity and the buoyancy scale.

Comparing the laws of motion of a vortex ring in a uniform ideal fluid [18], a uniform viscous fluid [15], and a stratified medium, we can note the following: in the first case, the circulation Γ, the translational velocity U, and the diameter of the ring D do not change during motion. In a viscous uniform medium, $D \sim t^{1/3}$, $U \sim t^{-1}$, $\Gamma \sim UD \sim t^{-2/3}$, $U \sim e^{-\beta x}$ [15]. In a stratified medium, the corresponding indices are functions of the initial Froude and Reynolds numbers. The vertical dimension of the ring is a nonmonotonic function of time or distance travelled. The wave resistance turns out to have the decisive effect on the dynamics of the ring at $Fr \lesssim 0.25$. The long life of spiral or annular striae with high values of the density gradient (which are not surfaces of vorticity concentration) is evidence of the suppression of mixing in the radial direction. At all stages of its existence, a laminar vortex ring remains symmetrical relative to the line of motion of its center.

LITERATURE CITED

1. A. T. Onufriev and S. A. Khristianovich, "Features of turbulent motion in a vortex ring," Dokl. Akad. Nauk SSSR, 229, No. 1 (1976).
2. V. A. Vladimirov and V. F. Tarasov, "Structure of turbulence near the core of a ring vortex," Dokl. Akad. Nauk SSSR, 245, No. 6 (1979).
3. A. T. Onufriev, "Features of vortical motion in the core of a vortex ring," in: Physical Mechanics. Dynamic Processes in Gases and Solids [in Russian], Vol. 4, Izd. LGU, Leningrad (1980).
4. T. Maxworthy, "Some experimental studies of vortex rings," J. Fluid Mech., 81, No. 3 (1977).
5. C. P. Wang, "Motion of a turbulent buoyant thermal in a calm stably stratified atmosphere," Phys. Fluids, 16, No. 6 (1973).
6. Ven H. Shui and Guy M. Weyl, "Motion of a rising thermal," Phys. Fluids, 18, No. 1 (1975).
7. A. M. Hecht, A. J. Bilanin, et al., "Turbulent vortices in stratified fluids," AIAA J., 18, No. 7 (1980).
8. A. M. Hecht, A. J. Bilanin, and J. E. Hirsh, "Turbulent trailing vortices in stratified fluids," AIAA J., 19, No. 6 (1981).
9. P. F. Linden, "The interaction of a vortex ring with a sharp density interface: a model for turbulent entrainment," J. Fluid Mech., 60, No. 3 (1973).

10. H. Honji and M. Tatsuno, "Vortex rings in a stratified fluid," J. Phys. Soc. Jpn., 41, No. 6 (1976).
11. V. I. Boyarintsev, A. I. Leont'ev, et al., "Propagation of vortex rings in a fluid of nonuniform density," Zh. Prikl. Mekh. Tekh. Fiz., No. 2 (1982).
12. J. C. S. Meng, "The physics of vortex ring evolution in a stratified and shearing environment," J. Fluid Mech., 84, No. 3 (1978).
13. V. N. Nekrasov and Yu. D. Chashechkin, "Measurement of velocity and the period of vibration of a liquid by the method of density markings," Metrologiya, No. 11 (1974).
14. V. I. Levtsov and Yu. D. Chashechkin, "High-sensitivity contact transducer for the electrical resistivity of a liquid and a device for its static calibration," in: Metrology of Hydrophysical Measurements. Summary of Documents of an All-Union Conference, VNIIFTRI, Moscow (1980).
15. T. Maxworthy, "The structure and stability of vortex rings," J. Fluid Mech., 51, No. 1 (1972).
16. R. H. Magarvey and C. S. Maclatchy, "The formation and structure of vortex rings," Can. J. Phys., 42, No. 4 (1964).
17. S. A. Makarov and Yu. D. Chashechkin, "Bound internal waves in a viscous incompressible liquid," Izv. Akad. Nauk SSSR, Fiz. Atmos. Okeana, 18, No. 9 (1982).
18. G. Lamb, Hydrodynamics [Russian translation], OGIZ, Moscow (1947).

AN INTENSE TURBULENT THERMIC IN A STABLY STRATIFIED ATMOSPHERE. NUMERICAL MODELING

Yu. A. Gostintsev and A. F. Solodovnik

UDC 536.253

Nonsteady-state convective turbulent flow due to climbing of a volume of liquid or gas with a deficit of density (a thermic) in an unrestricted medium has been theoretically studied in a number of works, which are reviewed in [1, 2]. These investigations allow one to qualitatively describe the gas-dynamic structure of the flow and the mechanism behind heat and mass exchange between the thermic and the surrounding medium. A study of these flows is complicated by the lack of data on the intensity of turbulent exchange in a thermic, which leads to arbitrariness in selecting the values for the coefficients of turbulent transfer. Here, the conditions required for adequate numerical modeling of a turbulent thermic are determined, and the dynamics of its climb from the moment of formation to that of height equilibrium in a stably stratified atmosphere are calculated.

1. Formulation of the Problem. The system of turbulence equations for describing axially symmetric, nonsteady-state convective flow of gas in a heat-concentrated thermic has the following form in the Boussinesq approximation:

$$\frac{\partial\Omega}{\partial t}+\frac{\partial}{\partial x}\frac{\Omega}{r}\frac{\partial\psi}{\partial r}-\frac{\partial}{\partial r}\frac{\Omega}{r}\frac{\partial\psi}{\partial x}=\frac{\partial}{\partial x}E\frac{\partial\Omega}{\partial x}+\frac{\partial}{\partial r}\frac{E}{r}\frac{\partial\Omega r}{\partial r}-\frac{\partial\omega}{\partial r},$$

$$\frac{\partial\omega}{\partial t}+\frac{\partial}{\partial x}\frac{\omega}{r}\frac{\partial\psi}{\partial r}-\frac{1}{r}\frac{\partial}{\partial r}\omega\frac{\partial\psi}{\partial x}=\mathrm{Pr}^{-1}\left(\frac{\partial}{\partial x}E\frac{\partial\omega}{\partial x}+\frac{1}{r}\frac{\partial}{\partial r}Er\frac{\partial\omega}{\partial r}\right)-\frac{N^2}{r}\frac{\partial\psi}{\partial r},\qquad(1.1)$$

$$\frac{\partial\vartheta}{\partial t}+\frac{\partial}{\partial x}\frac{\vartheta}{r}\frac{\partial\psi}{\partial r}-\frac{1}{r}\frac{\partial}{\partial r}\vartheta\frac{\partial\psi}{\partial x}=\mathrm{Pr}^{-1}\left(\frac{\partial}{\partial x}E\frac{\partial\vartheta}{\partial x}+\frac{1}{r}\frac{\partial}{\partial r}Er\frac{\partial\vartheta}{\partial r}\right)-\frac{N^2}{g\beta r}\frac{\partial\psi}{\partial r},$$

$$\frac{\partial\varepsilon}{\partial t}+\frac{\partial}{\partial x}\frac{\varepsilon}{r}\frac{\partial\psi}{\partial r}-\frac{1}{r}\frac{\partial}{\partial r}\varepsilon\frac{\partial\psi}{\partial x}=\mathrm{Sc}^{-1}\left(\frac{\partial}{\partial x}E\frac{\partial\varepsilon}{\partial x}+\frac{1}{r}\frac{\partial}{\partial r}Er\frac{\partial\varepsilon}{\partial r}\right),$$

$$\Omega=\frac{1}{r^2}\frac{\partial\psi}{\partial r}-\frac{1}{r}\frac{\partial^2\psi}{\partial r^2}-\frac{1}{r}\frac{\partial^2\psi}{\partial x^2},\quad\omega=g\frac{\rho_a-\rho}{\rho}\approx g\left[\beta\vartheta+\varepsilon\left(\frac{\mu_a}{\mu}-1\right)\right],$$

$$\Omega=\psi=\frac{\partial\omega}{\partial r}=\frac{\partial\vartheta}{\partial r}=\frac{\partial\varepsilon}{\partial r}=0,\ r=0,\ \Omega=\psi=\omega=\vartheta=\varepsilon\to0,\ r^2+x^2\to\infty.$$

Moscow. Translated from Zhurnal Prikladnoi Mekhaniki i Tekhnicheskoi Fiziki, No. 1, pp. 47-54, January-February, 1987. Original article submitted May 5, 1985.

0021-8944/87/2801-0043$12.50